NUCL SCI TECH (2021) 32:23
https://doi.org/10.1007/s41365-021-00859-1

Design of a 200-MHz continuous-wave radio frequency quadrupole accelerator for boron neutron capture therapy

Zhi-Chao Gao[1,2] · Liang Lu[3] · Chao-Chao Xing[1] · Lei Yang[1] · Tao He[1] · Xue-Ying Zhang[1,2]

Received: 16 September 2020 / Revised: 30 December 2020 / Accepted: 1 January 2021 / Published online: 13 March 2021

Abstract A high-intensity continuous-wave (CW) radio frequency quadrupole (RFQ) accelerator is designed for boron neutron capture therapy. The transmission efficiency of a 20-mA proton beam accelerated from 30 keV to 2.5 MeV can reach 98.7% at an operating frequency of 200 MHz. The beam dynamics have a good tolerance to errors. By comparing the high-frequency parameters of quadrilateral and octagonal RFQ cross sections, the quadrilateral structure of the four-vane cavity is selected owing to its multiple advantages, such as a smaller cross section at the same frequency and easy processing. In addition, tuners and undercuts are designed to tune the frequency of the cavity and achieve a flat electric field distribution along the cavity. In this paper, the beam dynamic simulation and electromagnetic design are presented in detail.

Keywords RFQ accelerator · BNCT · Dynamic simulation · Electromagnetic design

1 Introduction

As a cancer treatment method, boron neutron capture therapy (BNCT), which is a bimodal form of radiation therapy, was first proposed by the American scientist Locher in 1936 [1]. Because this approach requires drugs containing ^{10}B and an epithermal neutron beam that can kill tumor cells without affecting other tissues, a safe and stable neutron source is necessary.

Early BNCT experiments and clinical applications have used reactors as neutron sources, such as the Massachusetts Institute of Technology Reactor II [2] and the Tehran Research Reactor [3]. In recent years, with the development of strong current accelerator technology, BNCT neutron sources based on accelerators have been rapidly developed. Researchers have proposed a method for using an RFQ accelerator [4] to accelerate proton beams bombarding on targets to produce neutrons, which can be used as the front-end accelerator of AB-BNCT neutron source facilities [5]. For example, INFN (Istituto Nazionale di Fisica Nucleare) in Italy developed the TRASCO RFQ (TRAsmutazione SCOrie RFQ) for BNCT research [6]. INMRC (Ibaraki Neutron Medical Research Center) in Japan constructed a strong current proton accelerator which consists of a RFQ and a DTL for the same purpose [7]. These low-cost accelerator-based (AB) neutron sources with a compact structure are more suitable for use in hospitals.

A four-vane RFQ accelerator with an operating frequency of 200 MHz was designed in this study. The dynamic properties are presented in detail in the following section. In Sect. 4, we describe the electromagnetic design, including the cross section, tuners, and undercuts.

This work was supported by the National Natural Science Foundation of China (Nos. 11535016, 11675236, 12075296, 11775284)

✉ Liang Lu
luliang3@mail.sysu.edu.cn

[1] Institute of Modern Physics, Chinese Academy of Science, Lanzhou 730000, China

[2] University of Chinese Academy of Sciences, Beijing 100049, China

[3] The Sino-French Institute for Nuclear Energy and Technology, Sun Yat-sen University, Zhuhai 519000, China

2 Beam dynamic design

2.1 Requirements of BNCT

Beryllium or lithium is chosen as the target material of AB-BNCT neutron source in most cases. Although beryllium targets achieve a better thermal performance and mechanical properties, we chose to use lithium target because it requires a lower output energy for the accelerator. The reaction $^{7}\mathrm{Li}(p,n)^{7}\mathrm{Be}$ was selected to produce neutrons for BNCT because of its high neutron yield and relatively soft neutron energy spectrum, which can be used in BNCT clinical treatment with no significant slowing down. More considerations are involved in the design of lithium targets, which are not the focus of this paper and are not be discussed here.

According to the requirements of the International Atomic Energy Agency (IAEA) for clinical BNCT, the desirable minimum flux of epithermal neutrons (0.5 eV to 10 keV) is $10^{9}\,\mathrm{n/cm^{2}/s}$ [8]. The $^{7}\mathrm{Li}(p,n)^{7}\mathrm{Be}$ reaction has a threshold energy of 1.88 MeV and a remarkable resonance peak at 2.25 MeV for proton. It has a relatively low output energy for the RFQ, which makes it easier to design an RFQ and reduce the cost.

Considering the requirements of the IAEA and the characteristics of the reaction, Peking University has conducted a simulation showing that a 2.5 MeV proton beam with a current of 15 mA can fully meet the requirements for cancer treatment [9, 10]. Thus, a beam current of 20 mA was chosen with a final energy of 2.5 MeV.

Table 1 Main parameters of RFQ

Parameters	Value
Particle	H^{+}
Frequency (MHz)	200
Input energy (keV)	30
Output energy (MeV)	2.5
Current (mA)	20
Inter-vane voltage (kV)	91.65
Average aperture (mm)	5.406
R_{v}/R_{0}	0.75
Vane length (mm)	3162.62
Peak surface electric field (MV/m)	23.3774 ($K_{\mathrm{p}} = 1.59$)
Operation mode	CW
Transmission efficiency	98.7%

2.2 Beam dynamic parameters

The main parameters of the BNCT-RFQ are listed in Table 1. As indicated in Sect. 2.1, the particles to be accelerated, as well as the beam current and output energy, were determined. In addition, the frequency choice directly affects the size of the RFQ cavity, which is related to the cost of the construction. To reduce the occupied area and the construction cost of the RFQ to suit a hospital environment, the frequency is decided to be relatively higher, i.e., 200 MHz. The inter-vane voltage, which is related to the beam transmission efficiency and focusing effect, was determined to be 91.65 kV. Although the inter-vane voltage is relatively high, this parameter is considered reasonable. There are RFQs operating at higher inter-vane voltages. The LEDA RFQ in LANL has an inter-vane voltage ranging from 67 to 117 kV [11]. The IFMIF-EVEDA RFQ in LNL has a minimum voltage of 79 kV and a maximum voltage of 132 kV [12]. Meanwhile, the voltage ramp of the FRIB RFQ at Michigan State University ranges from 60 to 112 kV [13]. Portions of their operating inter-vane voltages are higher than 90 kV, which indicates that our design is reliable. A lower vane-gap voltage can improve the stability of the RFQ operation, but the length of the cavity, construction cost, and occupied area will increase. The other parameters listed in the table were determined through dynamic simulation.

2.3 Beam dynamic design

In this study, a dynamic transmission simulation was conducted using the software RFQGen [14]. Los Alamos National Laboratory (LANL) developed RFQGen based on the four-stage theory proposed by Stokes and Crandall [15], which allows the design of accelerating cells of the RFQ, including radial matching sections at both ends of the structure. The code can adjust the two-term potential functions by changing the vane geometry, thus generating both the accelerating force and the focusing force. Figure 1 shows the main parameters of the designed beam dynamics. When considering the shortest length and high transmission efficiency as the design goals, the length of this RFQ (acceleration proton beam of up to 2.5 MeV with an operating frequency of 200 MHz) is 3.2 m. Other similar RFQ accelerators are much longer, including the ADS-RFQ [16] in the Institute of Modern Physics in China (which operates at a frequency of 162.5 MHz and accelerates the proton beam from 35 keV to 2.1 MeV), which is 4.2 m, and the BNCT-RFQ [10] at Peking University (which operates at 162.5 MHz and provides acceleration of a 20-mA proton beam at up to 2.5 MeV), which is 5.2 m. The following figures show the simulation results for the beam dynamics. In Fig. 2, the transmission efficiency

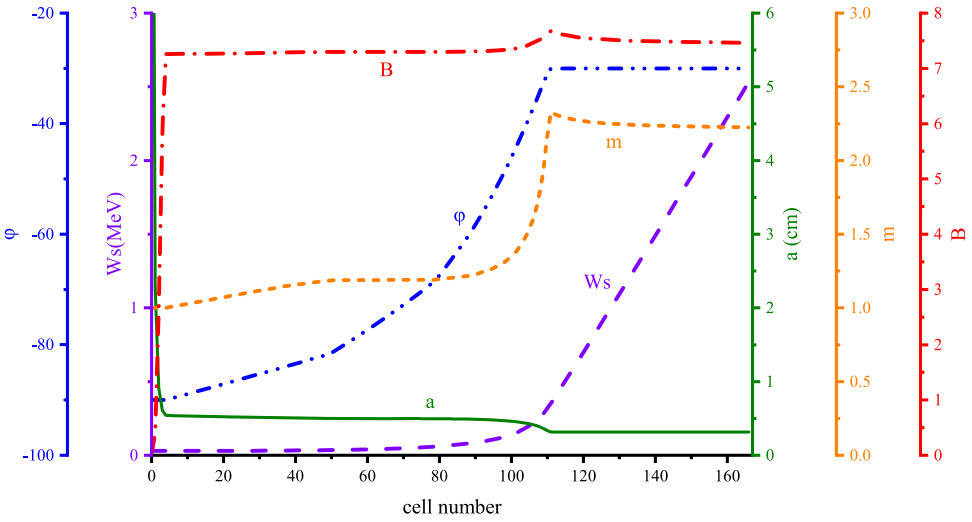

Fig. 1 (Color figure online) RFQ beam dynamic main parameters vary with accelerating cells

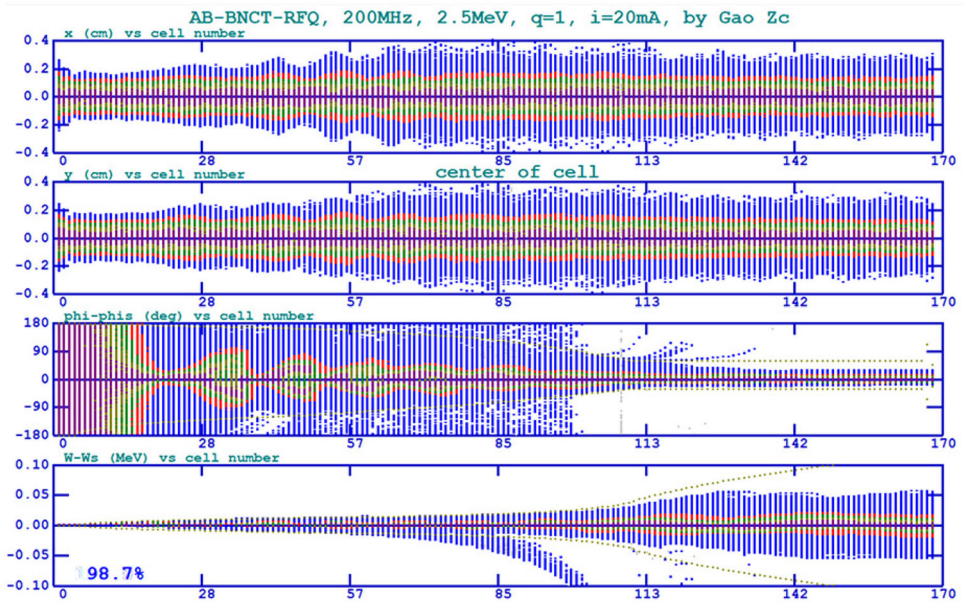

Fig. 2 (Color figure online) RFQ beam transmission process. There are beam envelope of the *X* axis and the *Y* axis, and the difference between particle phase and synchronous phase and energy spread, respectively

reaches 98.7% when 10,000 particles are simulated. In addition, Figs. 3 and 4 show the phase-space distribution and beam distribution at the entrance and exit of the RFQ.

2.4 Dynamic design tolerance

Only the ideal states of the parameters are considered in the dynamic transmission simulation. However, a slight disturbance will occur with the parameters when the beam travels from the ion source and low-energy beam transport line (LEBT) to the entrance of the RFQ. This may affect the transmission efficiency of the RFQ; thus, it is necessary to study whether the effect of the non-ideal matching conditions on the beam transmission efficiency is acceptable. Seven parameters (disturbance of input beam energy, current, voltage factor, normalized emittance, energy spread, Twiss parameters, and spatial displacements) were considered in this study. Figure 5 shows the results. The red triangles represent the designed parameters.

The input beam energy has an impact on the synchronous phase. Therefore, a deviation of the input energy may change the synchronous conditions, which leads to beam loss. As shown in Fig. 5a, the beam transmission efficiency is below 90% when the input energy is greater than 33 keV or less than 27 keV. The beam current is related to the space charge effects, which increase with the beam intensity. As shown in Fig. 5b, the beam transmission efficiency is over 98% as long as the beam current is lower than 30 mA. Figure 5c shows the change in beam transmission efficiency when the normalized voltage factor varies from 0.8 to 1.1, where a voltage factor of 1.00 indicates 91.65 kV. The beam transmission efficiency is

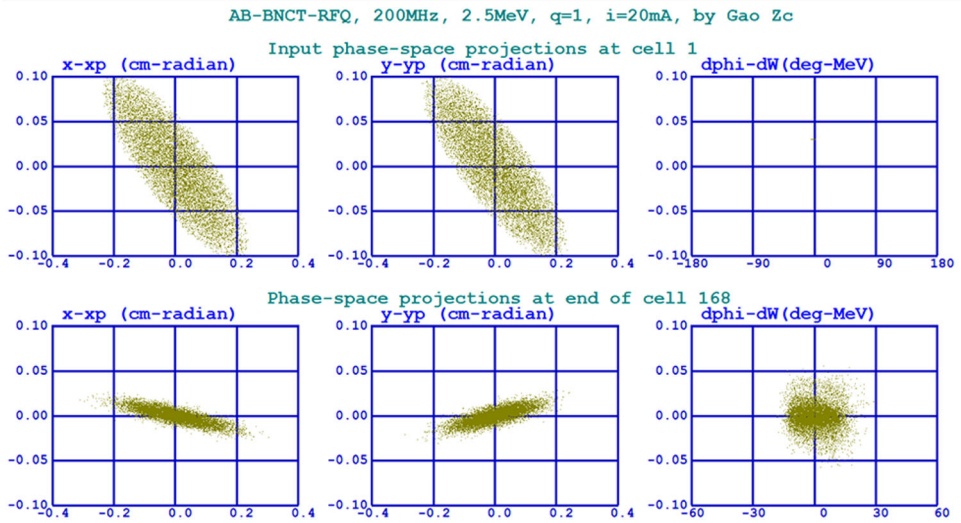

Fig. 3 (Color figure online) Beam profiles at the entrance and exit of the RFQ

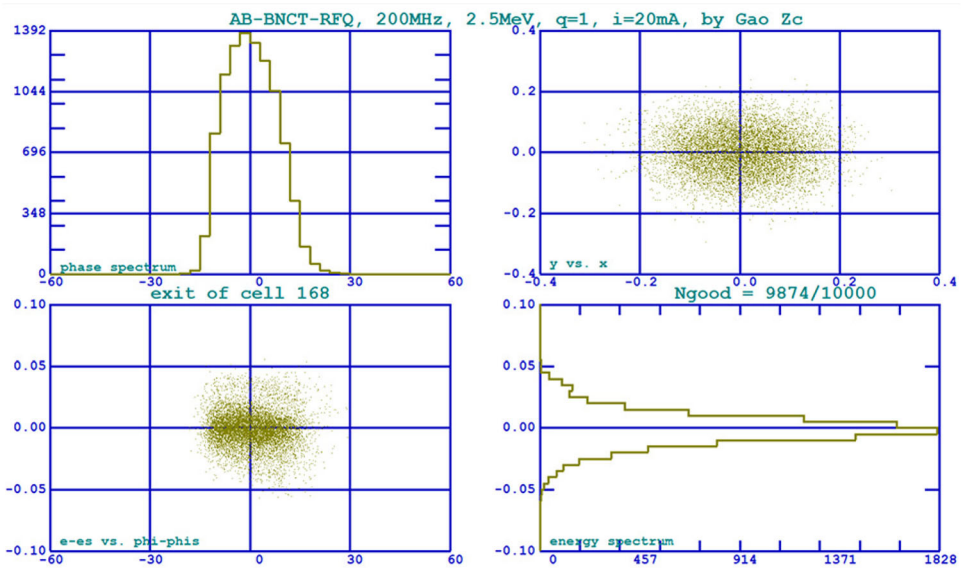

Fig. 4 (Color figure online) Beam distribution at the exit of the RFQ

acceptable if the vane voltage is 0.93-times higher than the designed voltage. Figure 5d shows the relationship between the normalized emittance of the beam and beam transmission efficiency. To ensure that the beam transmission efficiency is greater than 90%, the transverse emittance of the input beam should be no greater than 0.9 mm mrad. In addition, the beam transmission efficiency has sufficient margins for the beam energy spread, Twiss parameters, and beam spatial displacement, as shown in Fig. 5e–g. Overall, the parameters in Fig. 5 have a good margin for the beam transmission efficiency, which can guarantee a neutron flux for BNCT treatment.

3 Selection of cavity

Currently, the main cavity types of RFQ are four-vane RFQ [17–19] and four-rod RFQ [20–22]. The four-vane RFQ is suitable for accelerating light particles, such as protons and deuterons, and can operate under continuous-wave (CW) conditions. Compared with the four-rod RFQ, the four-vane RFQ has the advantages of a higher mechanical strength, lower power loss and power density, and simpler water-cooling structure. At the same frequency, the Q value of the four-vane RFQ cavity is larger

Fig. 5 (Color figure online) Effects of the **a** input energy, **b** input beam current, **c** normalized vane voltage, **d** normalized emittance, **e** energy spread, **f** Twiss parameters (α, β), **g** spatial displacements on the transmission efficiency ▶

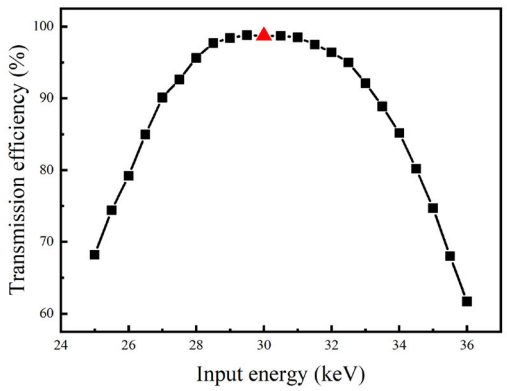
Transmission efficiency (%)
Input energy (keV)

(a)

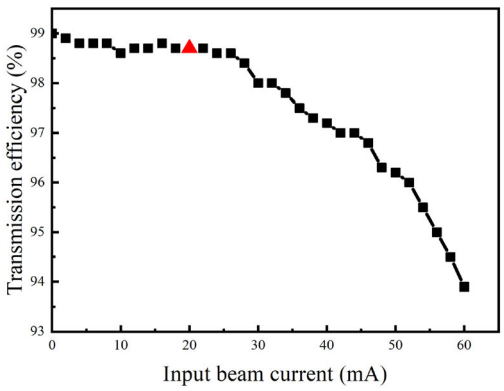
Transmission efficiency (%)
Input beam current (mA)

(b)

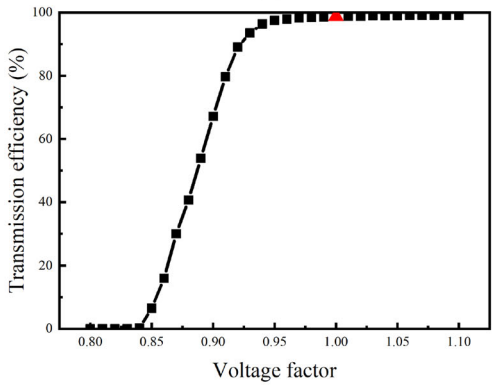
Transmission efficiency (%)
Voltage factor

(c)

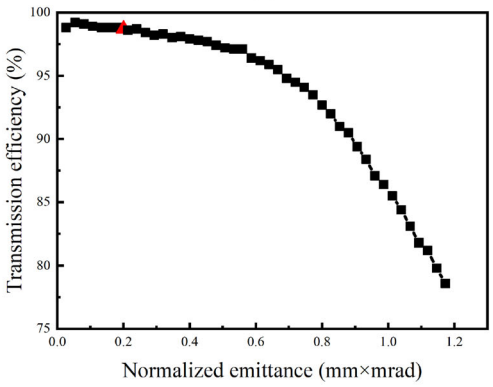
Transmission efficiency (%)
Normalized emittance (mm×mrad)

(d)

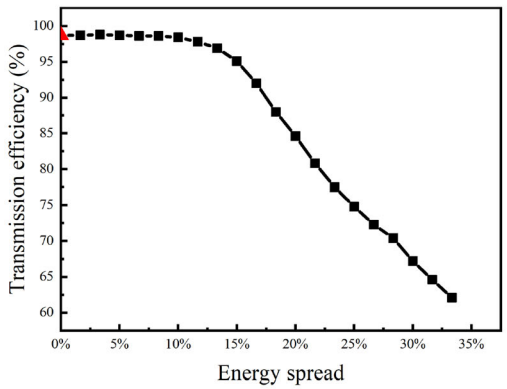
Transmission efficiency (%)
Energy spread

(e)

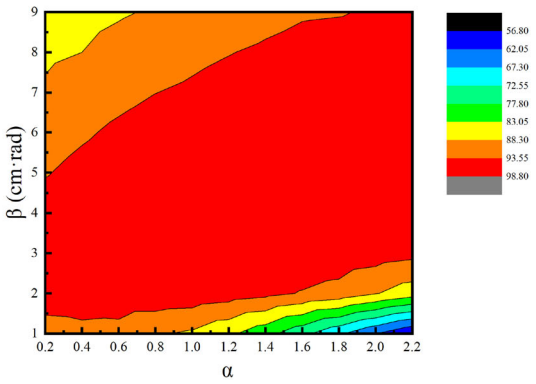
β (cm·rad)
α
56.80
62.05
67.30
72.55
77.80
83.05
88.30
93.55
98.80

(f)

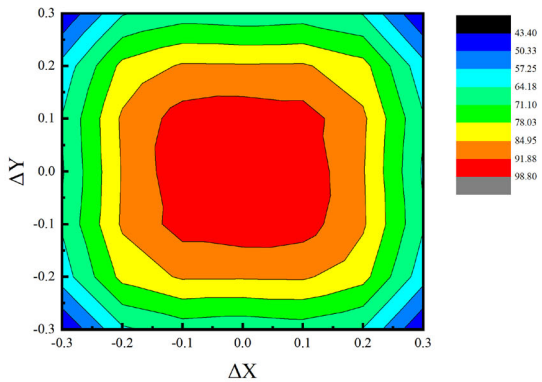
ΔY
ΔX
43.40
50.33
57.25
64.18
71.10
78.03
84.95
91.88
98.80

(g)

[23]. However, the four-vane structure has certain disadvantages, such as a large volume and high cost at low frequencies. For the AB-BNCT neutron source, the accelerator needs to operate in CW mode, considering that the cavity radius is approximately 15 cm after a preliminary simulation for a design frequency of 200 MHz, which is acceptable, and the four-vane RFQ is selected as the injector for the BNCT neutron source.

3.1 Quadrilateral cavity

A quadrilateral four-vane RFQ has a cross section similar to a square. Its right angles are replaced by arc angles to avoid point discharge and local over-temperature. Because the cross section is centrosymmetric, a quarter of the sketch is shown in Fig. 6a, which is determined using nine parameters. The values of the parameters determine the shape of the cross section. The values are presented in Table 2.

3.2 Octagonal cavity

The octagonal four-vane RFQ is an RFQ with a cross section similar to an octagon. From the sketch of the cross section, it is similar to the quadrilateral cavity except that the arc angles at the four peaks are replaced by straight lines, as shown in Fig. 6b. Table 2 lists the design parameters, which are similar to those of the quadrilateral cavity. Here, θ_3 is designed to have a larger value to reduce the power loss and local power density.

Table 2 Cross-sectional parameters of quadrilateral RFQ and octagonal RFQ

Parameter	Quadrilateral RFQ	Octagonal RFQ
R_0 (mm)	5.406	5.406
R_v ($= 0.75 \times R_0$) (mm)	4.05	4.05
L_1 (mm)	20	20
L_2 (mm)	20	20
θ_1 (°)	10	10
θ_2 (°)	10	10
θ_3 (°)	Null	22.5
R_c (mm)	30	30
R_w (mm)	40	Null
H (mm)	147.295	164.8

3.3 Comparison

To determine which type of cavity is better in terms of performance, a comparison of high-frequency parameters between the quadrilateral RFQ and octagonal RFQ is presented in Table 3, where Δf indicates the difference in frequency between the nearest quadrupole and dipole modes. The vane is made of copper and has an electrical conductivity of 5.8×10^7 S/m. To reduce the simulation time, we use the performance of a slice of the cavity instead of the entire RFQ cavity. For a more realistic simulation, the boundaries of the cross-profiles (lengthwise direction) were set as magnetic boundaries. The similar structure parameters, cavity frequency, and slice thickness of both types were designed in the same way. It is clear that

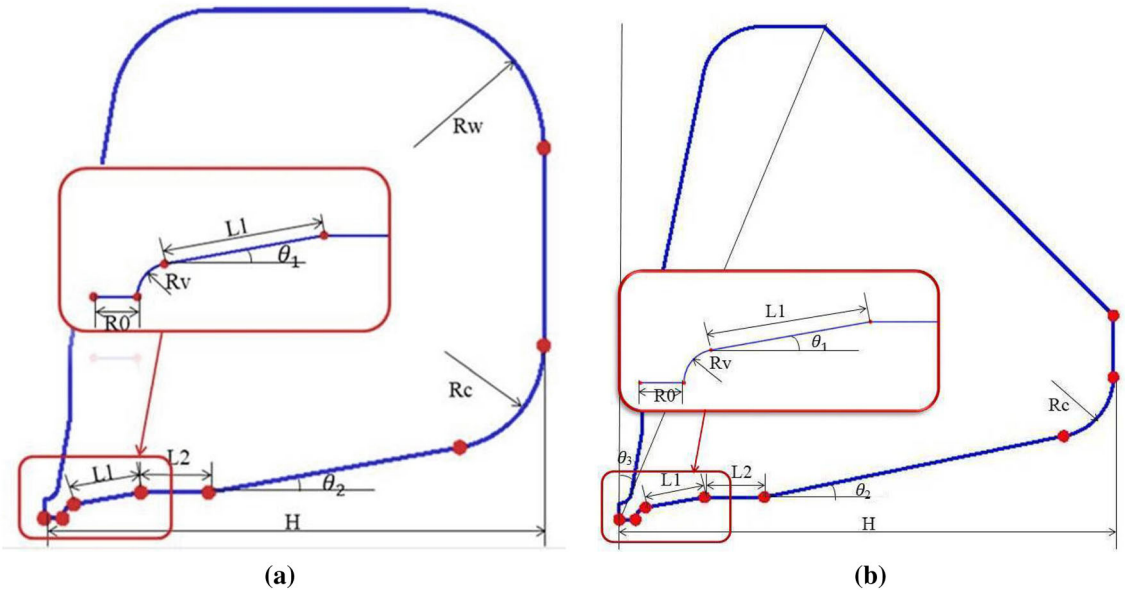

Fig. 6 (Color figure online) Cross sections of **a** quadrilateral RFQ, **b** octagonal RFQ

Table 3 Comparison of high-frequency parameters between quadrilateral and octagonal cavity

Parameter	Quadrilateral RFQ slice	Octagonal RFQ slice
Frequency (MHz)	200	200
Thickness (mm)	5	5
Δf (MHz)	6.36	6.35
H (mm)	147.295	164.8
Q	15715	14782
Total loss normalized to whole cavity (kW)	79.93	85.21

the values of Δf are both above 6 MHz. It is likely that neither requires a frequency separation structure. This is proved in the following section. From the perspective of the cavity size, H of the octagonal slice is 11.4% larger than that of the quadrilateral slice, which means that the cross-sectional area of the octagonal cavity is 13% larger than that of the quadrilateral cavity. A smaller size can reduce the costs of the construction and space. In addition, the quadrilateral slice has a higher Q value and less total RF loss. The cooling system for the quadrilateral cavity is easier to design and construct. Considering that the injector will be operated in CW mode, the quadrilateral RFQ cavity is a better choice.

4 Electromagnetic design

The goal of the EM design of the RFQ is to ensure that the frequency of the cavity meets the design frequency by adjusting the parameters or adding tuners and undercuts. It is also important to ensure that the electric field along the beam direction between the two opposite electrodes is flat. The frequency of the cavity and the spatial distribution of the eigenstates of the electric field are related to the shape of the cavity, that is, parameter H. The radio frequency (RF) structure design of the cavity is to elect the necessary eigenstate by finding out the spatial distribution of the field suitable for accelerating ion beam and then optimizing the size of the cavity to ensure that the cavity frequency meets the design frequency. The 3D code CST Microwave Studio [24] was used for the RF structure design of the RFQ. The parameters shown in Fig. 6a and Table 2 can be adjusted to optimize the high-frequency performance using MWS software.

4.1 Tuner design

The cylindrical structures shown in Fig. 7 are the tuners of the RFQ, and Table 4 shows the design parameters of the tuners. Tuners are used to slightly tune the overall resonant frequency of the cavity to keep the operating frequency of the cavity stable at the design frequency, or to adjust the local resonant frequency or electric field distribution of the cavity to achieve flatness of the electric field distribution along the cavity.

As shown in Fig. 7, the RFQ cavity has 64 tuners with a radius of 20 mm and a pre-insertion depth of 15 mm, uniformly distributed over the symmetrical electrodes. The effect of the tuners on the cavity frequency can be studied by adjusting the insertion depth of the tuners. According to Fig. 8, there is a linear relationship between the insertion depth and the cavity frequency, and the average sensitivity is 1 kHz/mm per tuner, that is, the tuning range of the whole cavity is − 0.92 to 1.0075 MHz.

As indicated in Sect. 3.3, there is no need for a frequency separation structure. This is proved in Sect. 4.3 after the whole-cavity simulation has been completed.

4.2 Undercut design

Another important task of an RF structure design is to tune the horizontal distribution of the electric field between electrodes along the longitudinal direction. The flat distribution of the electric field is extremely important for a frequency regulation during an operation. If the electric field is flat, when the depth of the tuner insertion or draw out is the same during the frequency regulation, the influence on the cavity voltage is also the same. The field distribution of the RFQ without undercuts is shown in Fig. 9. The electric field is low at both ends and high in the middle of the RFQ. The structure of undercuts is shown in Fig. 10, and Table 4 lists the design parameters of the undercuts. The undercut design generally adopts a triangular type, which has the advantages of high mechanical strength and convenient processing. By cutting off the conductor part and increasing the volume of the vacuum part, as shown in Fig. 9, the electric field distribution is flat along the longitudinal direction after adding the undercuts.

4.3 Whole-cavity simulation

Thus far, the design of the cross section and model of the RFQ cavity has been completed. To reduce the computing time, the electromagnetic structure design and

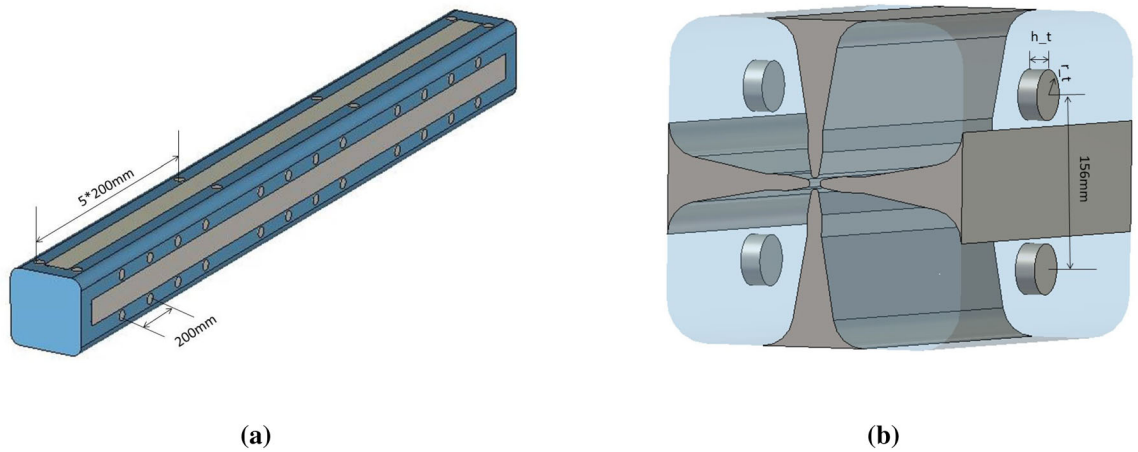

(a) (b)

Fig. 7 Design diagram of **a** whole cavity, **b** tuners

Table 4 Parameters of tuners and undercuts

Parameter	Value
Tuner	
r_t (mm)	20
h_t (mm)	15
Longitudinal interval between adjacent tuners (mm)	200
Tuner intervals in adjacent quadrants (mm)	156
Undercut	
h_{cut} (mm)	60
Theta (°)	60
D_{in} (mm)	75
D_{out} (mm)	68

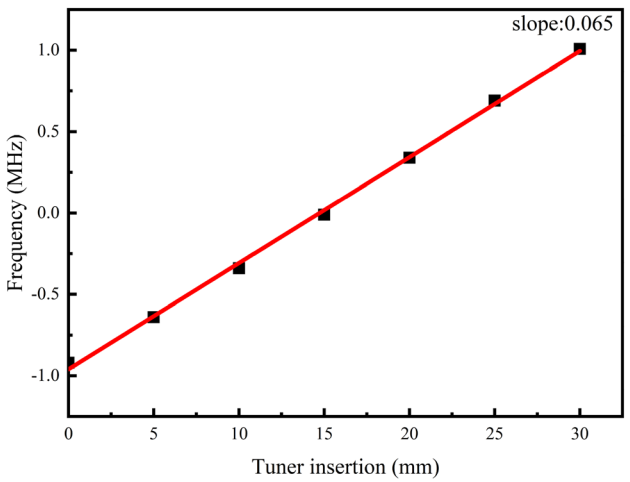

Fig. 8 Effect of tuner insertion depth on cavity frequency (for all tuners)

electromagnetic simulation described in this paper are all carried out using the average aperture R0 instead of the vane-tip modulation data generated by RFQGen software in the dynamic simulation, the results of which are similar. To increase the accuracy of the results and make the model more similar to a real RFQ, the electrodes were chamfered, and the modulations of RFQ were added to the model in the following whole-cavity simulation.

The RFQ cavity has 64 tuners, with a 3162.62-mm vane length and 3176.75-mm total length of the cavity and no frequency separation structure. The radial matching gap at the entrance of the RFQ (8.68 mm) and the fringe-field gap at the exit of the RFQ (5.45 mm) were added to the cavity. Both were determined using RFQGen software. CST software was used to simulate the entire cavity, and the K_p factor was found to be 1.69. The specific high-frequency parameters are listed in Table 5.

It is necessary to determine whether the dipole mode affects the normal operation mode of the RFQ because it will be excited if its frequency is close to the operation frequency. In the final whole-cavity RF simulation, as shown in Table 5, the minimum frequency interval Δf between the dipole mode and working quadrupole mode is 2.144 MHz. The Q value of the cavity was 14,361. According to references [23, 25], the effect of the dipole mode on the working quadrupole mode can be calculated through the following:

$$\alpha = 1/\sqrt{1 + \left(Q\frac{2\Delta f}{f_0}\right)^2} \tag{1}$$

where f_0 represents the operating frequency of the cavity, which was 200 MHz in this case. Thus, the value of α is 0.32%, which means that the nearest dipole mode has little effect on the operation mode. Therefore, there is no need for a mode separation structure.

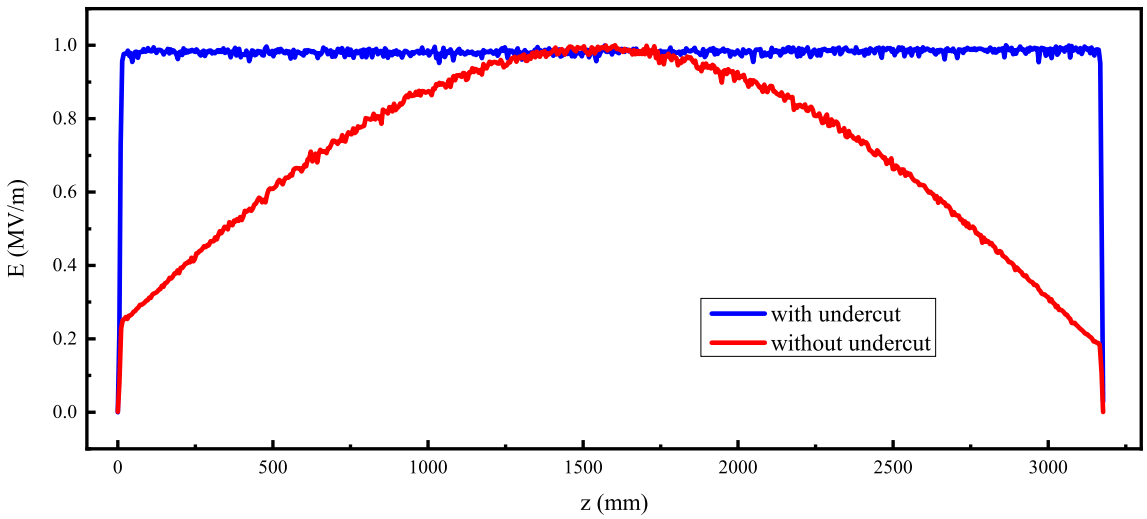

Fig. 9 Normalized electric field distribution between electrodes with and without undercut

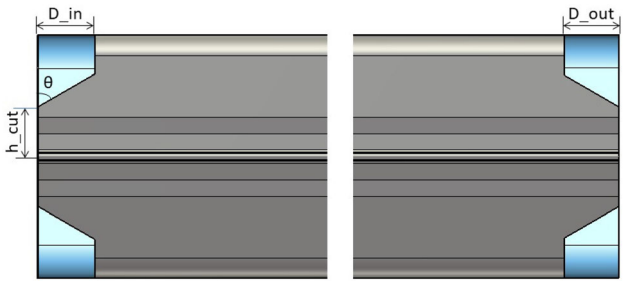

Fig. 10 Design diagram of undercuts

Table 5 RF parameters of whole-cavity RFQ

Parameter	Value
H (mm)	147.82
Frequency separation (MHz)	2.144
Q	14,361
Power loss (kW)	87.545

5 Conclusion

This paper takes the method of using RFQ to accelerate proton beam bombarding on lithium target to produce neutrons. The RFQ can be used as the front-end accelerator of AB-BNCT neutron source facility. The beam dynamic simulation of the RFQ was carried out using RFQGen software. At an operating frequency of 200 MHz, the transmission efficiency of a 20-mA proton beam accelerated from 30 keV to 2.5 MeV reached 98.7%, and the vane voltage and maximum surface field were controlled within a reasonable range. By studying the margins of the parameters of the accelerator, it is shown that the transmission efficiency of the RFQ can be maintained at above 95% under the condition that the parameters do not significantly change. For the RF structure design of the RFQ, the quadrilateral structure of the four-vane cavity was selected, which has the advantages of high mechanical strength, easy processing, simple water-cooling structure, and suitability for accelerating CW beams. In addition, to achieve the frequency regulation and field flatness regulation, tuners and undercuts were designed. Finally, the entire cavity with modulations and chamfers was simulated to meet the design requirements.

This paper mainly describes the design of the main body of the RFQ but does not consider the connection between the RFQ and front-end or back-end facility. For the RFQ design, it is also necessary to add the design of the coupler structure and perform a multi-physical field coupling analysis [26] and a secondary electron multiplication effect simulation.

Author contributions All authors contributed to the study conception and design. Material preparation, data collection and analysis were performed by Liang Lu and Zhi-Chao Gao. The first draft of the manuscript was written by Zhi-Chao Gao, and all authors commented on previous versions of the manuscript. All authors read and approved the final manuscript.

References

1. G.L. Locher, Biological effects and therapeutic possibilities of neutron. Am. J. Roentgenol. **36**, 1 (1936)
2. R.D. Rogus, O.K. Harling, J.C. Yanch et al., Mixed field dosimetry of epithermal neutron beams for boron neutron capture therapy at the MITR-II research reactor. Med. Phys. **21**, 1611–1625 (1994). https://doi.org/10.1118/1.597267

3. Y. Kasesaz, H. Khalafi, F. Rahmani et al., A feasibility study of the Tehran research reactor as a neutron source for BNCT. Appl. Radiat. Isot. **90**, 132–137 (2014). https://doi.org/10.1016/j.apradiso.2014.03.028
4. I.M. Kapchinskii, V.A. Teplyakov, A linear ion accelerator with spatially uniform hard focusing, 1–17 (1969)
5. T.P. Wangler, J.E. Stovall, T.S. Bhatia, et al., Conceptual design of an RFQ accelerator-based neutron source for boron neutron-capture therapy, in *Proceedings of the 1989 IEEE Particle Accelerator Conference*, vol. 1, pp. 678–680 (2002). https://doi.org/10.1109/PAC.1989.73220
6. P.A. Posocco, M. Comunian, E. Fagotti, A. Pisent, TRASCO-RFQ as injector for the SPES-1 project. Proceedings of Linac-66-68 (2004)
7. M. Yoshioka, T. Kurihara, S. Kurokawa et al., Construction of the accelerator-based BNCT facility at the IBARAKI Neutron Medical Research Center Proceedings of LINAC2014, 230–232 (2014)
8. IAEA, Current status of neutron capture therapy (2001). http://www-pub.iaea.org/MTCD/publications/PDF/te_1223_prn.pdf
9. B. Jeon, J. Kim, E. Lee et al., Target–moderator–reflector system for 10–30 MeV proton accelerator-driven compact thermal neutron source: conceptual design and neutronic characterization. Nucl. Eng. Technol. **52**, 633–646 (2020). https://doi.org/10.1016/j.net.2019.08.019
10. X.W. Zhu, H. Wang, Y.R. Lu et al., 2.5 MeV CW 4-vane RFQ accelerator design for BNCT applications. Nucl. Inst. Methods Phys. Res. A **883**, 57–74 (2018). https://doi.org/10.1016/j.nima.2017.11.042
11. L.M. Young, Simulations of the LEDA RFQ 6.7-MeV accelerator. Particle Accelerator Conference, pp. 2752–2754 (1997)
12. M. Comunian, A. Pisent, Legnaro, et al., The IFMIF-EVEDA RFQ: beam dynamics design, in *Proceedings of Linac* (2008)
13. N.K. Bultman, E. Pozdeyev, G. Morgan, et al., Design of the FRIB RFQ. Ipac (2015)
14. K.R. Crandall, T.P. Wangler, L.M. Young, et al., RFQ design codes. Los Alamos National Laboratory (2005)
15. R.H. Stokes, T.P. Wangler, K.R. Crandall, The radio-frequency quadrupole—a new linear accelerator. IEEE Trans. Nucl. Sci. **28**, 1999–2003 (2007). https://doi.org/10.1109/TNS.1981.4331575
16. Z.L. Zhang, H.W. Zhao, J. Wang, et al., Design of a four-vane RFQ for China ADS project, in *Proceedings of Linac* (2012)
17. J. Wei, H. Ao, N. Bultman, et al., FRIB accelerator: design and construction status, in *Proceedings of HIAT2015* (2015)
18. A. Ratti, R. DiGennaro, L. Doolittle, et al., Fabrication and testing of the first module of the SNS RFQ, in *International Linac Conference* (2000)
19. C.X. Li, Y. He, X.B. Xu et al., RF structure design of the China material irradiation facility RFQ. Nucl. Inst. Methods Phys. Res. A **869**, 38 (2017). https://doi.org/10.1016/j.nima.2017.06.045
20. A. Chakrabarti, V. Naik, O. Kamigaito et al., The design of a four-rod RFQ LINAC for VEC-RIB facility. Nucl. Inst. Methods Phys. Res. A **535**, 599–5 (2004). https://doi.org/10.1016/j.nima.2004.06.158
21. Q.F. Zhou, Z. Kun, Y.R. Lu et al., Simulation and experiments of RF tuning of a 201.5 MHz four-rod RFQ cavity. Chin. Phys. C **35**, 1042–1046 (2011). https://doi.org/10.1088/1674-1137/35/11/012
22. Z.S. Li, X.J. Yin, H. Du et al., The IH-RFQ for HIRFL-CSR injector. Nucl. Sci. Tech. **29**, 89 (2018). https://doi.org/10.1007/s41365-018-0416-y
23. W. Ma, L. Lu, X.B. Xu et al., Design of an 81.25 MHz continuous-wave radio-frequency quadrupole accelerator for low energy accelerator facility. Nucl. Inst. Methods Phys. Res. A **847**, 130–135 (2017). https://doi.org/10.1016/j.nima.2016.11.056
24. CST Studio Suite. http://www.cst.com
25. D.M. Pozar, *Microwave Engineering* (Wiley, London, 2011)
26. B. Zhao, B. Zhang, S.P. Chen et al., Multi-physics field coupling analysis of radio frequency quadrupole cavity. Nucl. Tech. **43**, 7–12 (2020). https://doi.org/10.11889/j.0253-3219.2020.hjs.43.030202 (**in Chinese**)